
A new possible model of sonoluminescence

Kravchenko M. B.

Department of Cryogenic Engineering, Odesa National Technological University,
112 Kanatna Street, 65039 Odesa, Ukraine kravtchenko@i.ua

Received: 08.01.2022

Abstract. We suggest a new theoretical model for the effect of sonoluminescence (SL). According to this model, conditions for a total internal reflection of light can be formed inside a collapsing gas bubble. Due to this, multiple reflections of visible light and infrared radiation occur at the inner surface of the bubble. After each reflection from the walls of the bubble, a slight decrease in the wavelength of thermal radiation takes place. We show on a specific example that only a few nanoseconds are enough to reduce notably the wavelength of thermal radiation inside the bubble. This model enables explaining the main features of the SL: a blackbody-like radiation spectrum with an extremely high temperature, a role of noble gases in increasing the SL intensity, and influence of water temperature on the SL intensity.

Keywords: sonoluminescence, luminescence, spectra, refractive index, noble gases.

UDC: 535.3

1. Introduction: basic experimental facts to be explained

Sonoluminescence (SL) is a phenomenon of light emission radiated from collapsing bubbles, which appears in some liquids under influence of sufficiently powerful ultrasonic waves. The first observation of SL has been made by M. Marinisco and Y. Y. Trillal [1] in 1933. They have described blackening of photographic plates as a result of emission that arises due to ultrasonic waves on water. In the next year, H. Frenzel and I. Schultes [2] have performed similar experiments and observed directly a glow of cavitation bubbles in the water. The SL emission spectrum has been obtained by P. Paounoff [3] in 1939, using a conventional spectrometer. Note that, due to a weakness of the emission, it took two days to expose the photographic plates. The emission spectrum of the SL has turned out to be continuous and close to that typical for a blackbody.

A significant progress in the SL studies has been witnessed after discovery of single-bubble SL effect. In this case, a single periodically cavitating bubble is being formed under the action of ultrasound, instead of a multitude of randomly appearing and disappearing bubbles. In 1989, a then graduate student F. Gaitan working under the direction of L. Crum at the University of Mississippi, has created a device in which a standing acoustic wave is excited inside a glass bulb [4]. They have managed to select the power and the frequency of ultrasonic waves in such a way that only one stable bubble is being formed in the centre of the flask, which is visible to a naked eye [5]. In 1992, F. Gaitan et al. [5] have developed an experimental method for recording individual flashes of light during pulsation of a single cavitation bubble in a cylindrical resonator chamber.

In the same 1992, R. Hiller et al. [6] have studied the emission spectra for the single-bubble SL. It has turned out that the SL spectrum for the case of a bubble cavitating in water is continuous and fits well into the shape of ‘tail’ of a blackbody radiation. Under normal conditions, the

emission originated from a gas bubble corresponds to the blackbody temperature 25000 K. Furthermore, the emission spectrum corresponds to an essentially higher temperature, 50000 K, when the water temperature drops down to 10°C.

The studies of bubble dynamics have testified that, with sinusoidal changes in the acoustic pressure, stable pulsations of the bubble are observed only starting from certain threshold amplitude of ultrasonic vibrations. Moreover, when the amplitudes of the acoustic pressure become close to the threshold, the periods of expansion and contraction of the bubble are the same and no SL is observed. As the amplitude of ultrasonic vibrations increases, the change in the bubble radius becomes substantially nonlinear. It is in this nonlinear mode that the SL can only be observed.

It is understood that the sound wave with a sufficiently high power in the under-pressure phase breaks a continuous medium. Then a small bubble is being created in the medium which is filled with water vapour and gases dissolved in water. After half of the period, in the compression-wave mode, this bubble collapses under the influence of external pressure and surface-tension forces, though it does not disappear at all. A flash of light bursts out when a minimal bubble radius is reached. At the last stage of bubble collapse, the velocity of its walls can become as high as $\sim 4M$ (i.e., 1300 m/s, with M being the Mach number) [7]. A flash of light occurs at this stage in less than 1 ns.

Interesting and important results have been obtained in the studies of influence of noble gases dissolved in a liquid on the intensity of single-bubble SL. These studies have been carried out by R. Hiller et al. in 1994 [8]. The review [9] reports the spectra of the single-bubble SL obtained upon saturation of water with various noble gases at the partial pressure equal to 400 Pa. Here the main features remain the same for all the noble gases. Namely, the intensity of the emission arising from the cavitation bubble increases with increasing molar mass of the dissolved noble gas. Moreover, this result is valid for both the water and the other liquids for which the SL has been investigated.

Studies of the influence of helium isotopes ^3He and ^4He on the SL have been of especial importance. A significant change in the SL intensity achieved upon saturation of water with these gases indicates that the intensity is influenced by the molar mass of dissolved gas. A further progress in the understanding of single-bubble SL has been achieved owing to the studies of the effect for 85% sulphuric-acid solution in water. The most important advantages of this experimental technique are as follows. (i) The SL in the sulphuric-acid solution appears to be much brighter than that in the pure water. Under the same conditions, the intensity of the single-bubble SL observed in the case of sulphuric-acid solution saturated with argon becomes 2700 times higher, if compared with the effect observed in the water saturated with argon [10]. (ii) The sulphuric-acid solution has a very low saturated vapour pressure and, moreover, it remains transparent to the ultraviolet radiation down to the wavelength 200 nm.

Simultaneously with the single-bubble SL, its multi-bubble counterpart has also been elucidated. With the multi-bubble SL, the critical ultrasound power can be achieved in a relatively large volume of water and, due to this fact, many (e.g., hundreds of) cavitation bubbles are generated in the vacuum phase of vibration, instead of a single bubble. The above studies have demonstrated that the spectra of emitted light obtained in this mode differ notably from those peculiar for the single-bubble SL.

T. J. Matula et al. [11] have compared for the first time the spectra of the single- and multi-bubble SLs referred to 0.1 M NaCl solution in water. Separate emission lines have been observed in the spectra of the multi-bubble SL. In a more detail, there is the emission line of electronically excited hydroxyl OH^* (310 nm) and the line of Na^+ ion. It is worthwhile that these lines have not

been detected with the single-bubble SL. Y. T. Didenko and T. V. Gordeychuk [12] have also observed the emission lines of hydroxyl OH* at 310 nm when studying the spectra of the multi-bubble SL in the water saturated with noble gases. The presence of separate emission lines in the case of multi-bubble SL and their absence in the single-bubble emission mode under the same conditions indicate to significant differences in the mechanisms of light emission responsible for these two SL modes. The above differences in the properties of single- and multi-bubble SLs have even given rise to a hypothesis that the appropriate luminescence mechanisms are fundamentally different [13, 14].

The situation has become even more confusing after publication of the work by J. B. Young et al. [15] who have reported observation of individual emission lines in the spectrum referred to the single-bubble SL. The authors have detected the emission lines of hydroxyl OH* with the wavelength 310 nm under a reduced acoustic pressure of ultrasound, as well as a very weak single-bubble SL in the water saturated with argon. Later on, K. S. Suslick and D. J. Flannigan [16] have observed the separate emission bands of argon in the spectrum of single-bubble SL, which occur in the 85% solution of sulphuric acid saturated with argon. Due to a higher SL intensity for this solution, detailed SL spectra under a reduced ultrasound power have been obtained.

It has been noted that the intensity of the SL decreases with decreasing amplitude of ultrasonic vibrations and clear emission bands of argon atoms appear. Conversely, the argon emission lines become expanded with increasing acoustic pressure and completely disappear when the acoustic pressure reaches the value 0.5 MPa. These emission spectra have made it possible to calculate the gas temperature inside the cavitation bubble in two different ways. First, this can be done issuing from the continuous spectrum of a blackbody radiation and, second, the temperature of atomic argon can be calculated from a specific set of its spectral lines and their intensities. The appropriate calculations have been performed using the well-known energy levels of electrons in argon atoms, the probabilities of transitions among the corresponding electronic levels and the energies of the emitted photons.

The authors [16] have also noted that the argon emission spectrum contains the bands that point to a large population of the energy states with very high excitation energies (more than 13 eV). The excitation of these states is extremely unlikely at the temperatures of the order of 10000 K. It would require the temperatures higher than 100000 K – or the particles (e.g., electrons) with sufficiently high energies – to provide a noticeable population of the energy states mentioned above.

W. B. McNamara et al. [17] have examined the emission spectra of the multi-bubble SL in silicone oil saturated with argon or helium. The authors have noticed a slight ‘red’ shift of the emission bands associated with Cr(CO)₆ and Mo(CO)₆ dissolved in silicone oil. In all the experiments performed with silicon oil saturated with argon, the red shift turns out to be greater than the effect observed when it is saturated with helium. Earlier, D. Kuhns et al. [18] have investigated the multi-bubble SL in the 1 M aqueous solution of NaCl and have also found a red shift of the emission lines of Na⁺ ions, when compared with the emission of a flame containing NaCl.

The effect of red shift in the emission spectra of atoms and molecules occurring during the SL has been explained in different ways by different authors. For instance, M. A. Margulis [14] has believed that this effect cannot be caused by increased pressure inside the bubble and explains it by a Rayleigh shift towards the ‘red’ region, which takes place during the scattering of radiation in water. The authors [16, 17] have admitted that there are no theoretical prerequisites for

explaining the red shift of lines in the SL spectrum by a high gas pressure inside the bubble. Nevertheless, they explain this effect precisely by high pressure and temperature of the gas inside the cavitation bubble and refer a reader to the experimental results concerned with gas compression where a similar red-shift effect has been observed.

The above review of the main experimental facts in need of explanations does not claim to be complete. Its only purpose is outlining the range of problems that still have no consistent explanations. This is why we have mentioned only the most famous and typical experimental works as the illustrations of these unsolved problems.

2. SL models

The two groups of models are currently used to explain the SL: thermodynamic models and models of electrical-breakdown channels. The main argument in favour of the thermodynamic theories is that the SL spectrum is usually continuous and, moreover, it is described well as a blackbody radiation in the visible range. In the frame of thermodynamic SL models, a gas heated during bubble's collapse is considered as a light source. Various thermodynamic models differ in the ways along which the gas is heated. Currently, most of the researchers in the field adopt a simple model of adiabatic compression and a shock-wave model. In the adiabatic-compression model, the light is emitted by a gas heated to a high temperature due to its adiabatic compression.

The first thermodynamic model, the model of adiabatic compression, suggested for the SL in 1950 is due to B. E. Noltingk and E. A. Neppiras [19, 20]. The authors of the model have analyzed the conditions arising inside a collapsing bubble and concluded that the temperatures of about 10^4 K can be reached during adiabatic compression of a gas inside a bubble. To their opinion, the glow arising during adiabatic compression of a bubble is nothing but the equilibrium radiation of a heated gas.

The authors of the works [19, 20] have used a so-called Rayleigh–Plesset equation to describe the radial motion of the surface of the cavitation bubble under the action of a sound wave. This equation can be written as

$$R\ddot{R} + \frac{3}{2}\dot{R}^2 = \frac{1}{\rho} \left[\left(P_0 + \frac{2\sigma}{R_0} \right) \left(\frac{R_0}{R} \right)^{3\gamma} - \frac{2\sigma}{R} - \frac{4\mu\dot{R}}{R} + P_\infty \right], \quad (1)$$

where R is the bubble radius, ρ , σ and μ denote respectively the density, the surface tension and the viscosity of a liquid, γ stands for the adiabatic index for the gas filling a bubble, R_0 the bubble radius under (initial) ambient conditions, P_0 the fluid pressure, and P_∞ the acoustic pressure. Note that the l. h. s. of Eq. (1) describes the inertial properties of the bubble and its r. h. s. gives the resulting force acting upon the bubble surface. In particular, the expression

$$\left(P_0 + \frac{2\sigma}{R_0} \right) \left(\frac{R_0}{R} \right)^{3\gamma} \quad (2)$$

gives the gas pressure arising inside the bubble when its radius changes from R_0 to R . In this case, the model of adiabatic compression of an ideal gas is used to describe the behaviour of gas inside the cavitation bubble. In addition to the properties of the gas and the density of the liquid, Eq. (1) takes into account the forces of surface tension and viscous friction in the liquid. Finally, the change in the bubble radius is understood to occur under the action of a variable acoustic pressure P_∞ .

Generally, the Rayleigh–Plesset equation describes adequately the changes in the radius of cavitation bubble that take place under the action of ultrasonic wave. This can be illustrated by

comparing the measured radiuses of the cavitation bubble with the calculated ones. A noticeable discrepancy between the calculations and experiments arises only when the density of the gas inside the bubble becomes comparable to the density of the liquid.

Numerous attempts have been made to improve the Rayleigh–Plesset equation by taking into account a variable mass of saturated vapours inside the bubble, using a known van der Waals equation to describe the properties of the gas filling the bubble, and taking compressibility of the liquid into consideration [14]. However, the attempts to account for even some of these effects make the Rayleigh–Plesset equation too complex. As a consequence, the only possible numerical solutions of this equation have not yet provided reliable values of the maximal temperature and pressure inside the cavitation bubble [14].

When simulating dynamics of the cavitation bubble, no one has paid a due attention to considering the heat transfer with the surrounding liquid. Perhaps, this is because the collapse of the bubbles occurs very quickly and, therefore, the process of gas compression inside the bubble is usually considered as adiabatic. To estimate the rate of unsteady thermal conductivity of a body, the Fourier criterion (in dimensionless time) is commonly used:

$$F_o = \frac{a \tau}{R^2}, \quad (3)$$

where R is the characteristic size of a body (in our case, the radius of the bubble), τ the time of the heat-transfer process, and a the thermal diffusivity of a body (in our case, the gas filling the bubble). The thermal diffusivity of the gas inside the bubble can be found as

$$a = \frac{\lambda_g}{C_p \rho_g}, \quad (4)$$

where λ_g denotes the thermal conductivity of the gas, C_p its heat capacity under constant pressure and ρ_g its density.

If a uniformly heated solid sphere is placed into a liquid, the temperature in its centre, after a while, would be practically equal to the temperature on its surface. The problem of unsteady heat conduction occurring at a constant temperature of the surface of sphere has been solved analytically [21]. The solution is such that the degree of completeness of heat transfer inside a heated solid sphere can be estimated whenever the value of the Fourier criterion is known. Let us consider a uniformly heated sphere, of which initial temperature is 100 K higher than that of the surrounding liquid. Then the value of the Fourier criterion must be greater or equal to 0.4 in order to cool this sphere so that the temperature in its centre would be less than 2 K higher than the temperature at its periphery [21]. In other words, the process of unsteady heat transfer for the solid sphere is practically completed when the Fourier-criterion values are greater than 0.4.

Let us find the characteristic cooling time of an argon-filled bubble placed in a liquid. The thermal conductivity of argon at the pressures from 0.1 to 40 MPa and the temperature 300 K can be taken from the reference book [22]. Setting the value of the Fourier criterion equal to 0.4 and the radius of the argon bubble equal to 1, 5 and 10 μm and substituting the values of the thermal diffusivity of argon into Eq. (3), one can find the appropriate characteristic times of the process of bubble cooling. Fig. 1 shows the dependences of characteristic cooling time on the argon pressure inside the bubble under different conditions. Using the data reported by S. J. Putterman and K. R. Weninger [7], we estimate the characteristic time of collapse of the cavitation bubble as 5 μs .

Comparing this time with the characteristic cooling times taken from Fig. 1 for the gas bubble, one can become convinced that the time required for equalizing the temperatures inside the

cavitation bubble is much shorter than the time of bubble collapse. Hence, the process of gas compression inside the cavitation bubbles is much closer to isothermal rather than adiabatic compression, although the latter is usually incorporated in the Rayleigh–Plesset model. Therefore, reaching the temperatures of the order of 10^4 K inside the cavitation bubble is, in principle, impossible. Indeed, while the gas is being compressed, it would have enough time to cool down to a temperature close to that of the surrounding liquid.

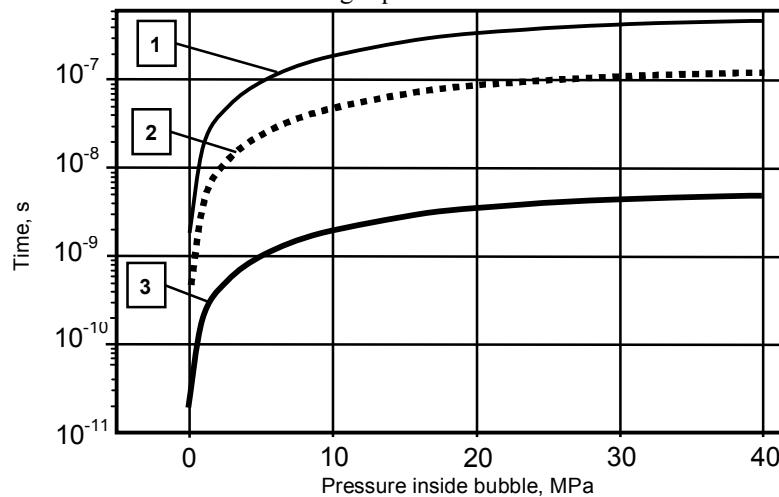


Fig. 1. Dependences of cooling time for an argon bubble on the pressure: curves 1, 2 and 3 correspond respectively to the values of Fourier criterion equal to 0.4. 1, 2 and 3 (the bubble radiuses 10, 5 and 1 μm)

Another argument in favour of the fact that the emission of light during the SL is not thermal is a short duration of the light pulse (about 1 ns). In other words, the duration of the light pulse is much shorter than the time during which the collapse of the gas bubble occurs (5–10 μs). If the radiation had a thermal nature, then it would be possible to observe a smooth increase in the temperature of gas inside the bubble and a corresponding increase in the intensity of the glow. In any experiments, however, just the opposite behaviour is observed: a short and bright flash of light occurs at the moment when the radius of the cavitation bubble reaches its minimum.

To explain the above experimental results, it is necessary to assume a faster compression of the gas inside the bubble. This serves as a basis for the shock-wave model adopted for explanation of the SL. It has been shown theoretically that formation of a shock wave inside the bubble is possible in the water–air system. According to the model, formation of the shock waves moving towards the centre of the bubble is assumed at the last stage of compression, which lasts for ~ 5 –10 ns [14]. A convergence of the shock waves to the centre of the bubble and their reflection from the centre leads to compression of the gas to high pressures and its heating to high temperatures. At the moment of reflection, a high-density core of ionized gas is formed. After reflecting from the centre, a diverging shock wave is formed, which quickly ‘quenches’ the radiation due to decreasing gas temperature.

The shock-wave model is also controversial. According to the calculations [23], the radius of the high-temperature zone is an order of magnitude smaller than the minimal bubble radius, and the lifetime of such a high-temperature zone is 10^{-13} – 10^{-11} s. Still this is inconsistent with the experimental data obtained by K. Weninger et al. [24]. On the other hand, studies have been conducted concerning a space-time irregularity of the single-bubble SL emission, using colour filters. It has been found that the angular irregularity of the emission is practically absent in the

‘red’ spectral region (i.e., at the wavelengths $\lambda > 500$ nm), although there is a noticeable angular irregularity of the SL intensity in the ‘blue’ region ($260 < \lambda < 380$ nm). This demonstrates that the size of luminous region is comparable to the radiation wavelength transmitted by a red filter (~ 500 nm). The latter complies fairly well with the data of direct measurements of the minimal bubble radius, though is much larger than the size of the luminous region given by the shock-wave model. Finally, despite a large number of experimental and theoretical works reported up to date on the model of shock waves, the existence of such waves inside a cavitation bubble has not yet been proven directly.

The electric models of the SL emission are based on different mechanisms of separating electric charges, which generates an electric field, the strength of which is sufficient for electric breakdown in the gas filling the bubble. Most of these models have still remained at the level of hypotheses. Almost all the electrical models of SL are based on the assumption that bubble collapse is asymmetric and, due to this, a charge separation occurs. In Ref. [25], the SL-light source is sparking discharges around a water jet, which are formed at the end of the bubble-collapse process. These can be electrical discharges separated in cracks formed in the water when a gas jet collides with bubble walls [26]. The electrical-breakdown models of the SL can successfully explain a short duration of the light flash and a high temperature of the glowing plasma. On the other hand, these models are usually criticized because of inconclusive explanations of the causes and the magnitudes of the electric charges separated inside the cavitation bubble.

Summarizing our discussion, we conclude that the most important question concerned with the problem of SL is the nature of appropriate radiation source. To explain the main bulk of the available experimental results, only two thermodynamic models are mainly considered in the literature: the model of adiabatic compression and the shock-wave model. However, none of these models describes the entire set of the experimental data [14]. In other terms, although the SL effect has been known for more than 80 years and a lot of new information has been accumulated after decades of its intense experimental studies, an entirely self-consistent and non-contradictory explanation of the effect is still absent.

3. Refractive index of a compressed gas

In view of a hypothesis about the SL nature we wish to put forward, the refractive index of the gas that fills the cavitation bubble becomes of fundamental importance. When the refractive index of the gas inside the bubble is higher than that of the surrounding liquid, a total internal reflection of visible (or infrared) light inside the bubble becomes possible. Our calculation results will demonstrate that, at the end of the bubble-collapse process, the refractive index of the gas inside the bubble can indeed become higher than the refractive index of the surrounding water.

To calculate the refractive index of a compressed gas, a standard Lorentz-Lorentz formula is usually used, which relates the refractive index of a gas with the polarizability of its atoms or molecules. When light passes through a transparent medium under the action of alternating electromagnetic field, only electron shells of atoms are displaced with respect to their nuclei. Due to their larger inertia, heavier atomic nuclei cannot respond to a rapidly changing electromagnetic field of the visible or ultraviolet radiation. Then the Lorentz–Lorentz formula works well, which takes into account only electronic polarizability of atoms and molecules. If the transparent substance consists of non-polar atoms or molecules, the latter formula reads as follows:

$$\frac{n^2 - 1}{n^2 + 2} = \frac{4\pi}{3} N\alpha, \quad (5)$$

with n implying the refractive index, N the molecular density of the substance and α the polarizability of molecules of the substance. Sometimes it is more convenient to rewrite Eq. (5) in the form

$$\frac{n^2 - 1}{n^2 + 2} \frac{M}{\rho} = \frac{4\pi}{3} N_A \alpha, \quad (6)$$

where M is the molar mass of the substance, ρ its density and N_A the Avogadro number.

The results of experimental studies of the refractive index of gaseous nitrogen at the pressures up to 40 MPa have been reported in Ref. [27]. It has been shown there that the Lorentz–Lorenz formula describes well the refractive index of nitrogen up to 40 MPa, since the dependence of the refractive index on the gas density is practically linear. As a result, a simple empirical formula has been suggested for the refractive index of nitrogen:

$$n = 1 + 0.264\rho_N, \quad (7)$$

where ρ_N is the nitrogen density in $[\text{g}/\text{cm}^3]$ [27].

The formulae suitable for calculating the refractive index of water and water vapour as a function of temperature, pressure and light wavelength have been given in Ref. [28]. Moreover, the work by C. T. Wanstall et al. [29] has compared various formulae used when calculating the refractive indices for mixtures of different substances at the temperatures and pressures close to their critical values. It has been demonstrated that the best results can be obtained with a so-called additive polarization model. The appropriate Lorentz–Lorenz formula adapted for the refractive indices of mixtures of substances acquires the following form [29]:

$$\frac{n^2 - 1}{n^2 + 2} = \rho_{MIX} \sum_k \alpha_i X_i. \quad (8)$$

Here ρ_{MIX} stands for the molar density of a mixture, which takes the properties of real gases into account, α_i is the polarizability of molecules of the i -th component of this mixture, and X_i the molar concentration of the i -th component.

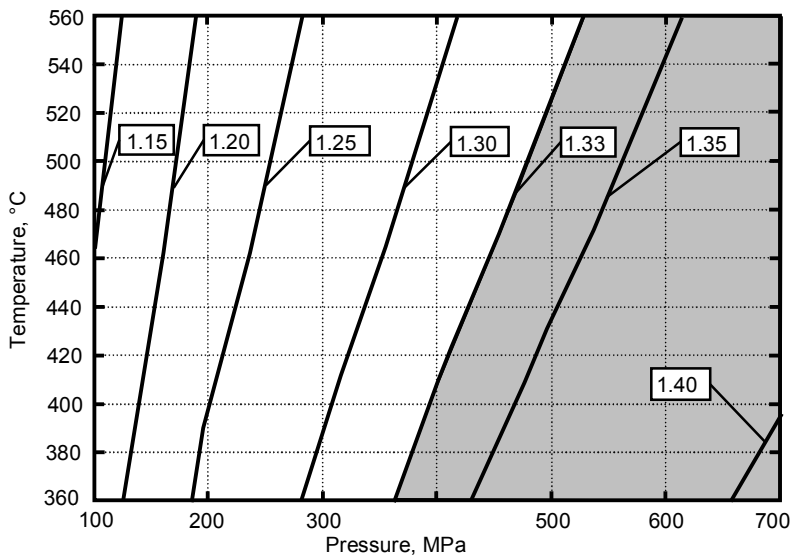


Fig. 2. A diagram of refractive indices, as calculated for a 50% mixture of water vapour and nitrogen at different temperatures and pressures: solid lines correspond to refractive-index values indicated in the legend. The area where the refractive index of the gas filling the bubble is higher than the refractive index $n = 1.33$ of surrounding water is highlighted in gray.

Fig. 2 displays the refractive index of the mixture of water vapour and nitrogen calculated at different temperatures and pressures. The molar concentration of nitrogen in the mixture is taken to be equal to 50%. The polarizabilities of water vapour and nitrogen have been taken from Refs. [27, 28]. Finally, we note that our calculations use the model of additive polarization. The area in which the refractive index of the mixture filling the gas bubble is greater than the refractive index of water (equal to 1.33) is highlighted in gray. The main conclusion is as follows: the states of the gas inside the cavitation bubble, in which its refractive index becomes higher than the refractive index of the water surrounding this bubble, are indeed possible, although they can occur only at very high pressures that exceed 400 MPa.

Of course, any direct measurements of the pressure inside the cavitation bubble are not feasible with the current state of experimental apparatus and techniques. Therefore, this pressure can be estimated only theoretically, basing on the solutions of Rayleigh–Plesset equation. Depending on the adopted set of assumptions, different maximal gas pressures inside the bubble have been obtained. For the case of adiabatic compression, the Rayleigh–Plesset model gives the pressures of the order of 3500–6000 MPa at the end of bubble-collapse process [30]. This is much higher than the minimal pressure that provides the refractive index of the gas being higher than that of water. Notice also that D. J. Flannigan et al. [30] have estimated the pressure reached inside the cavitation bubble as being greater than 370 MPa.

Cavitation is accompanied not only by light emission but also by destruction of the surfaces which the cavitation gas bubbles come into contact with. This gives rise to formation of cavities on the surface of propellers in high-speed vessels and damage to the sealing elements of hydraulic valves. The tensile strength of the materials of which the propellers are made is 500–600 MPa. Therefore, to detach metal particles from the surface of such a material, a gas pressure higher than 500–600 MPa is required inside the cavitation bubble. Hence, there are both theoretical and experimental data indicating that the pressures inside the cavitation bubbles can be high enough to provide the situation when the refractive index inside the bubble becomes higher than the refractive index of the surrounding liquid.

The studies of dynamics of the diameter of a single cavitation bubble have testified that, at the last stage of bubble collapse, the velocity of movement of its boundary can exceed the speed of sound in the gas filling the bubble [9]. In this case, a shock wave should emerge ahead of the bubble boundary. The pressure inside the volume where the shock wave exists is several times higher than that in the central part of the bubble. This can explain the effect of the molar mass of noble gases dissolved in a liquid on the SL intensity.

The intensity of the SL increases with increasing molecular weight of the noble gases in which the water or the other liquid is saturated. This can be interpreted as a result of two factors that reinforce each other. Below we will show that the SL intensity is the higher, the earlier the refractive index of the gas filling the bubble becomes higher than the refractive index of the surrounding liquid. The first factor of saturation of the liquid with heavy noble gases lies in increasing refractive index of the mixture of gases that fill the cavitation bubble. It is known that increasing molar mass of a noble gas induces an increase in the refractive index of this gas. For example, the refractive indices of helium, neon, argon, krypton and xenon under atmospheric pressure amount respectively to 1.000035, 1.000067, 1.000284, 1.000472 and 1.000702. Consequently, substituting increasingly higher mixture densities and larger polarizabilities of the noble gases into Eq. (8) would result in significantly higher refractive indices for the mixtures doped with heavier noble gases. As a second factor, saturation of the liquid where the SL is

observed with heavy noble gases imposes a decrease in the sound speed for the mixture of gas and vapour that fill the cavitation bubble. For instance, the speed of sound under normal conditions is respectively equal to 965, 435, 319, 224 and 178 m/s in helium, neon, argon, krypton and xenon.

Therefore, the rate of bubble collapse, at which the velocity of its walls reaches the speed of sound in the gas filling this bubble, will be reached in less time in the bubble filled with heavier noble gases. This can explain a significant difference in the SL intensities obtained at the saturation of water with ^4He and ^3He isotopes. These helium isotopes differ only in their molar masses, whereas all the other properties are almost identical. Due to different molar masses, the speed of sound in these gases is notably different. Namely, the speed of sound in ^4He is less and the shock wave would appear earlier in the process of bubble collapse. Consequently, it would take a less time to achieve the pressure at which the refractive index of the gas filling the bubble becomes higher than that of the surrounding liquid.

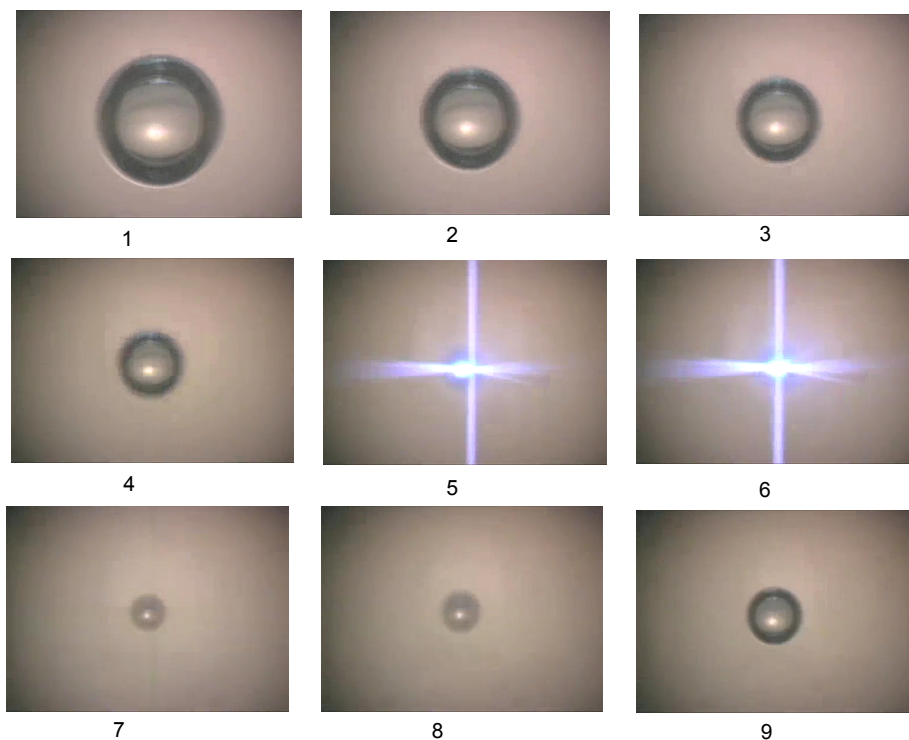


Fig. 3. A series of sequential frames taken from a high-speed video recording of SL effect [31].

To confirm the hypothesis that the optical properties of the filling gas would change during the collapse of the cavitation bubble, let us analyze a publicly available high-speed video recording of SL [31]. Fig. 3 displays a series of consecutive frames taken from this video. In particular, frames 1–4 in Fig. 3 demonstrate how the diameter of the bubble decreases. Here the bubble looks like air bubbles in water. There is an area in the bubble centre where the light is reflected from. It then enters a camera lens. A dark rim can be seen along the border of the bubble, where the light is also reflected. However, this reflected light does not enter the camera lens because of too large angles of light incidence, so that this part of the bubble looks darker.

Frames 5 and 6 in Fig. 3 show a bright SL flash arising from the area which is much smaller than the sizes of the bubbles in the previous frames. One can see from frames 7 and 8 how the gas

bubble increases in size gradually but, this time, it looks radically different from the bubble seen in the previous frames. Here a round gray area with a uniform density is visible. Finally, one can see in frame 9 that the bubble has become larger, while its optical properties have radically changed and become similar to those observed in frames 1–4.

The changes in the optical properties of the cavitation bubble seen from Fig. 3 can be explained as follows. When the pressure and the temperature inside the bubble become such that the refractive index of the gas filling the bubble becomes higher than that of the surrounding liquid, the gas bubble begins to work as a convex lens. In the place where the gas bubble is situated, an enlarged image of the gas in the focus of this lens is seen in the corresponding frames. Following from the data of Fig. 3, one can conclude that the state of the gas inside the cavitation bubble, where the refractive index is higher than that of the surrounding liquid, lasts less than the time interval between the two adjacent frames. Since about 187 frames pass between the two flashes of light, and the ultrasound frequency ensuring the SL is usually 20–30 kHz, one obtains the time interval between the two adjacent frames amounting to 0.2–0.3 μ s. Hence, the state of the gas, in which the refractive index of the latter is higher than the refractive index of the liquid surrounding the bubble, lasts less than 200–300 ns.

4. Relativistic Doppler effect

From the standpoint of our model, it looks relevant to remind of a relativistic Doppler effect. It manifests itself as a change in light wavelength occurring due to relative motion of light source and its receiver. With consideration of the relativistic effect of time dilation, the effect is described within the special theory of relativity. Namely, the influence of the time dilation on the wavelength change can be taken into account by introducing a Lorentz factor into a classical formula for the Doppler effect. When the source and the receiver move directly towards each other, the wavelength change due to the relativistic Doppler effect reads as [32]

$$\frac{\lambda_r}{\lambda_s} = \frac{1 - \frac{v}{c}}{\sqrt{1 - \left(\frac{v}{c}\right)^2}} = \sqrt{\frac{1 - \frac{v}{c}}{1 + \frac{v}{c}}}, \quad (9)$$

where λ_r implies the wavelength measured by the receiver, λ_s the wavelength emitted by the source, v the speed of mutual movement of the source and receiver, and $1/\sqrt{1 - \left(\frac{v}{c}\right)^2}$ the Lorentz factor.

Fig. 4 illustrates a scheme of the effect of total internal light reflection occurring inside a cavitation gas bubble. If the refractive index of a gas inside a bubble is higher than the refractive index of a liquid surrounding this bubble, then the total internal reflection of light can be observed. The relevant condition is that the incidence angle at the inner border of the bubble must be greater than the critical angle. Let the refractive index of the gas filling the cavitation bubble be 1.40. This is quite realistic from the viewpoint of the above calculations (see Fig. 2). When the refractive index of water is taken to be 1.33, the critical angle φ of the total internal reflection of light inside the gas bubble is given by

$$\varphi = \arcsin\left(\frac{1.33}{1.40}\right) = 71.8 \text{ deg} . \quad (10)$$

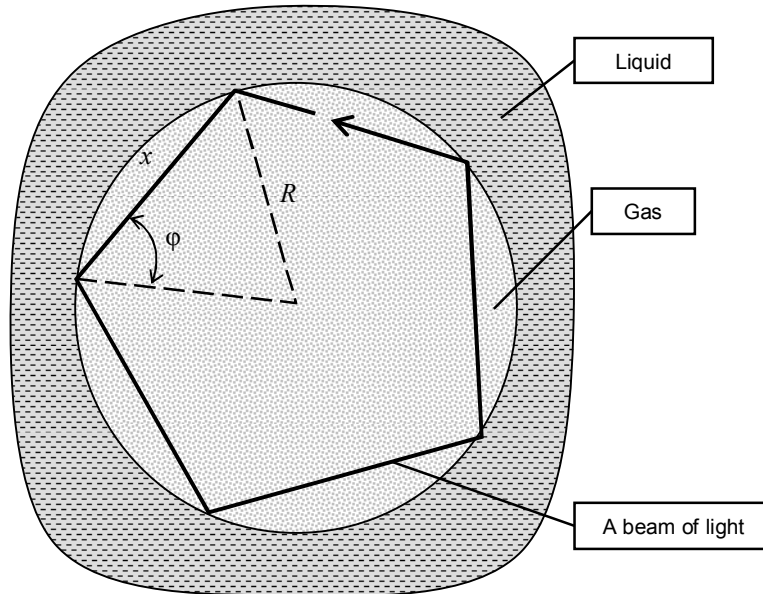


Fig. 4. A scheme of total internal reflection of a light beam inside a compressed gas bubble.

If the radius of the cavitation bubble and the critical angle of total internal reflection are known, one can easily determine the distance passed by the light between its two successive reflections. Let the incidence angle be exactly equal to the critical angle. Then this distance can be found as

$$x = 2R \cos(\phi) . \quad (11)$$

If the diameter of the gas bubble decreases rapidly, the points at which the light is reflected inside the bubble will become nearer to each other. This is equivalent to the situation when the radiation source and the receiver inside the bubble move towards each other.

Let the velocity of the bubble boundary be equal to v_0 and the conditions of total internal reflection be fulfilled. Then the radiation sources and its receivers inside the bubble come together with the velocity

$$v = \dot{x} = 2\dot{R} \cos(\phi) = 2v_0 \cos(\phi) , \quad (12)$$

where v_0 is the speed of boundary of the cavitation gas bubble and v the speed at which the sources and receivers approach each other inside the bubble. Since the speed of light is much greater than the speed of the bubble walls, the change occurring in the incidence angle at the inner surface of the bubble during the pass of light between the two successive reflections can be neglected. Using the refractive index of the gas filling the cavitation bubble, one can determine the speed of light inside it:

$$c_g = \frac{c}{n} = \frac{3 \times 10^8}{1.4} = 2.14 \times 10^8 \text{ m/s}, \quad (13)$$

with c being the speed of light in a vacuum. As shown above, the state of the gas in which its refractive index is higher than the refractive index of the liquid surrounding the bubble lasts less than 200–300 ns.

Now we will demonstrate that even the time interval of 6 ns during which the gas stays in this state is enough for a flash of light to appear. Knowing the speed of light inside the cavitation bubble, one can find that a 6 ns-long travel of light inside the bubble corresponds to the distance

1.29 m. Having set the average bubble radius of 2 μm and using Eq. (11), we obtain the path length 1.26 μm run by the light between the two successive reflections from the inner walls of the bubble. Knowing the total path length of light inside the bubble and the average distance between the two successive reflections, we find the total number of light reflections inside the bubble. It turns out to be 1.02×10^6 .

Let us set the speed of motion of the walls of the cavitation bubble to be 1.3 km/s, which agrees with the results of direct measurements of the time dependence of the bubble radius [9]. Then the light wavelength should decrease by only $3.55 \times 10^{-4}\%$ after the two successive reflections of light from the walls of the collapsing bubble. As a result of 1.02×10^6 reflections from the inner walls of the bubble, which occur in 6 ns, the radiation wavelength should decrease by the factor of 37.4. From the physical point of view, this means that the mechanical energy of the collapsing bubble is transferred to the thermal radiation inside it, which leads to decreasing wavelength of this radiation.

Let us consider the question of how the multiple reflections of thermal radiation from the moving walls of the gas bubble would affect the energy spectrum of this radiation. In the case of blackbody radiation, the dependence of spectral power density on the frequency ω is described by a standard Planck formula [33], which can be written as

$$\frac{dP}{d\omega} = \frac{\hbar\omega^3}{\pi^2 c^2} \frac{1}{\exp\left(\frac{\hbar\omega}{kT}\right) - 1}. \quad (14)$$

Here P denotes the power emitted by a single surface of a blackbody, h the Planck constant, k the Boltzmann constant and T the absolute temperature.

The spectral density of the blackbody radiation has a maximum, of which position depends only on the temperature:

$$\frac{\hbar \omega_{\max}}{kT} = 4.9651. \quad (15)$$

The consequence is that, due a Doppler frequency shift, the radiation spectrum of a blackbody preserves its character, though the corresponding temperature increases as much as the radiation frequency has increased. Notice that a well-known Wien's displacement law, which relates the wavelength λ_{\max} of the maximum intensity of thermal radiation to the absolute temperature of a blackbody, strictly follows from Eq. (14) [33]:

$$\lambda_{\max} = \frac{2898 \times 10^3 [\text{nm}]}{T[\text{K}]}. \quad (16)$$

Let us now assume that the temperature of the gas compressed inside the cavitation bubble is 400 K. Then the wavelength of thermal radiation inside this bubble, which corresponds to its maximum intensity, is equal to 7245 nm. After the bubble has collapsed, the wavelength corresponding to the maximal intensity decreases by 37.4 times and becomes equal to 194 nm, which corresponds to the temperature of about 15000 K.

When the collapsing bubble reaches its minimal radius, the shape of the bubble ceases to be spherical, the incidence angle of light at the inner surface of the bubble becomes less than the critical angle of total internal reflection, and the light finally escapes from the bubble. A confirmation of this phenomenon can be seen in frame 5 of Fig. 3. Here the first flash of light is asymmetric with respect to the centre of the collapsing bubble. Thus, one can explain the appearance of a short bright flash of light at the moment when the radius of the collapsing bubble

reaches its minimum. The above ‘blue-shift mechanism’ suggested by us for the emission spectrum of a collapsing bubble is compatible with the fact that the SL spectrum has a blackbody character and, moreover, it also explains a seemingly unrealistically high temperatures inside the bubble.

Our mechanism for increasing energy of thermal-radiation quanta also enables explanation of paradoxical results obtained in the work [16], where the bands of argon emission spectrum have been analyzed for the case of single-bubble SL. Namely, a significant (if compared with the ground state) population of the excited, very high-energy (of the order of 13.3 eV) states have been found in Ref. [16]. The authors of the work [16] rightly point out that the population of these levels is not of a thermal origin, since the temperature 15000 K would have corresponded to the energy 1.3 eV of thermal motion.

Another paradoxical result of the work [16] is the emission lines of ionized oxygen molecules O_2^+ observed in the SL spectrum. It is known that the binding energy of atoms in the oxygen molecule amounts to 5.1 eV, while the ionization energy of the molecule is 12.1 eV. Therefore, excitation of ionized oxygen molecules could not be thermal because the oxygen molecules should have already decayed at the temperatures necessary for this. On the other hand, our hypothesis implies that, under certain conditions, a decrease in the wavelength of thermal radiation can occur inside the collapsing gas bubble, with no increase in the temperature of the gas filling the bubble. Consequently, the excitation of such high-energy levels in the molecules of gases is indeed not thermal but occurs when the short-wavelength radiation is absorbed.

In addition, the suggested mechanism of the blue shift taking place in the thermal-radiation spectrum can offer a simple explanation of why the SL intensity becomes significantly increased in the liquids saturated with noble gases. Let us elucidate this point in a more detail. First, the molecules of all the noble gases do not have vibrational energy levels, since they consist of single atoms. Most of the vibrational transitions occurring in the molecules of di- or tri-atomic gases correspond to the wavelength range 2.5–25 μm , with is compatible with the infrared range (0.5–1000 μm). Therefore, due to vibrational levels in poly-atomic gas molecules, their infrared spectra contain many absorption bands corresponding to vibrational transitions.

When a quantum of thermal radiation approaches the energy of one of these vibrational levels after a series of successive reflections inside the collapsing bubble, there is a high probability that it will be absorbed by a molecule of poly-atomic gas. The energy of the absorbed quantum can either dissipate in small portions and turn finally into heat – or become reradiated as a quantum with the same or less energy. Therefore, the presence of poly-atomic gases inside the collapsing bubble leads to a significant weakening of SL. Conversely, filling the collapsing gas bubbles with the noble gases reduces absorption and thermalization of the infrared quanta inside the bubbles.

The latter phenomena can also explain the increase in the SL intensity that happens with decreasing water temperature. Since the water vapour represents a tri-atomic gas, it has a number of absorption bands in the infrared range. The density of the water vapour inside the cavitation bubble decreases exponentially with decreasing temperature of the water, which implies increasing intensity of the SL. The monograph [8] provides the experimental dependence of the relative SL intensity as a function of temperature of the water saturated with various noble gases. As a matter of fact, this dependence represents a straight line on the semi-logarithmic scale in the temperature region 10–50°C.

The dependence of the partial pressure P_{H_2O} of saturated water vapour on the temperature has the form [22]

$$\begin{aligned}
 P_{H_2O} &= P_{T_0} \exp\left(-\frac{Q_{H_2O}}{RT}\right) = P_{T_0} \exp\left(\frac{-Q_{H_2O}}{R(273.15+t)}\right) \\
 &\approx P_{T_0} \exp\left[\left(\frac{-Q_{H_2O}}{273.15 \cdot R}\right)\left(1 - \frac{t}{273.15} + \dots\right)\right],
 \end{aligned}
 \tag{17}$$

where P_{T_0} is a constant measured in the units of pressure, Q_{H_2O} the molar heat of vapourization for the water, R the universal gas constant, and T and t denote respectively the temperatures in Kelvins and degrees Celsius. In a general case, the molar heat of vapourization of water depends also on the temperature, although it can still be considered as a constant in a small enough temperature region. Moreover, only the first term of a series can be left in Eq. (17) in this region, whereas the rest of the terms can be neglected. Taking logarithms of the r. h. s. and l. h. s. of Eq. (17), one obtains a function of which plot represents a straight line on the semi-logarithmic scale:

$$\ln\left(\frac{P_{H_2O}}{P_{T_0}}\right) = \left(\frac{-Q_{H_2O}}{273.15R}\right)\left(1 - \frac{t}{273.15}\right).
 \tag{18}$$

Hence, the dependence of SL intensity on the water temperature coincides with the temperature dependence of the pressure of saturated water vapour, up to a constant factor.

5. Luminescence of gas placed inside a collapsing bubble

Let us remind some basic notions and facts to be discussed further on in this Section. When a gas molecule has absorbed a photon, the energy of the latter can excite one of electrons of this molecule to a higher energy level. A reverse transition of electron to its relaxed (ground) state can also occur, which is accompanied by releasing of energy. The latter can be freed both in parts, thus turning into heat, and in a single portion, i.e. in the form of photon. The luminescence of molecules represents a spontaneous emission, the power of which is excessive with respect to the equilibrium thermal radiation at a given temperature, while the duration of luminescent radiation is much longer than the period of the corresponding oscillations. Note that the excited states of molecules are relatively stable. If absorption of a photon by a molecule occurs in a time of the order of 10^{-15} – 10^{-14} s, then this molecule can be excited for about 10^{-9} – 10^{-8} s before finally emitting a photon and returning to its ground state.

We also remind that, under certain conditions arising during the collapse of a gas bubble, its mechanical energy can be transferred into thermal radiation filling this bubble. As a result, the total energy of the photons inside the bubble increases and they can be absorbed by the molecules of gases and vapours filling the bubble, thus switching these molecules into their excited states. Finally, it has been found in all the experimental SL studies that the shape of the flare is not symmetrical. Namely, the leading edge of the flash is steeper, being well described by Gaussian error function, while its decay is flatter, being described in the best manner by exponential function [13].

According to the hypothesis put forward by us, the thermal radiation circulates and becomes more intense along the walls of the collapsing gas bubble. Within the region of incidence angles greater than the critical angle of total reflection, the exact directions of the rays are random. This can be caused by even the slightest deviations from the spherical shape of the bubble, fluctuations in the gas density inside the bubble, and diffraction of light. As a consequence, the fact that the leading edge of the SL flare arising at the extreme point of bubble collapse is well described by the Gaussian error function is quite natural.

A slower dropdown in the SL intensity can be explained by the fact that the luminescence of excited gas molecules inside the bubble is added to the light from the flash itself. This idea is supported by the following considerations. First, since the probability of transition to the ground state is the same for all electrons located at a certain energy level, the luminescence intensity decreases exponentially with time, which is typical for decaying of the SL flare. Second, separate bands in the spectra of both single-bubble and multi-bubble SLs have been detected in a number of experimental studies (see Refs. [11, 15]). A presence of these bands in the SL spectra makes it possible to determine not only which kind of molecules emit light, but also which electronic levels are excited in these molecules [16].

The experimental studies of dynamics of the radius of cavitation bubble and the SL intensity demonstrate that the flash of light occurs just at the endpoint of the collapse of the gas bubble, and most of gentle decline in the intensity of this flash falls on the phase of bubble expansion [7]. If we assume that the luminescent emission of excited gas atoms occurs in the region of flare-intensity decay, this can explain the known ‘red’ shift of the peaks in the SL spectra.

Fig. 3 indicates that, even after the SL flash has gone out, the refractive index of the gas filling the bubble can remain larger than that of the liquid surrounding this bubble. A sharp change in the optical properties of the bubble seen in the last frame 9 evidences this assumption. Then a mechanism can be at work which is the same as the mechanism leading to the ‘blue’ shift of thermal radiation inside the collapsing bubble. However, the appropriate spectrum shifts towards the red side since the bubble expands. The expansion rate is much less than the rate of collapse of the bubble, so that the ‘red’ shift of peaks in the luminescence spectrum is much smaller than the ‘blue’ shift of thermal radiation during the bubble collapse.

There is another difference between the shift in the emission spectrum during expansion of the bubble and the corresponding shift occurring during its collapse. It is associated with the fact that the angle of light incidence on the walls of this bubble (i.e., the angle φ in Fig. 4) slightly increases with decreasing size of the gas bubble. Therefore, the total internal reflection of light inside the collapsing bubble should be ensured for any number of internal reflections. When the bubble expands, the opposite result is obtained: the angle of light incidence on the inner walls of the bubble slightly decreases after each reflection until it becomes less than the critical angle. After that, a portion of light would penetrate through its walls and leave the bubble. This can explain the asymmetry of the spectral SL peaks, which has been pointed out by D. J. Flannigan and K. S. Suslick [35]. In particular, specific plots have been presented in this study, which illustrate a ‘red’ shift, a broadening and an asymmetry of argon emission line in the case of single-bubble SL, when compared with the emission of a mercury–argon lamp taken as a reference.

Since any luminescence represents a spontaneous emission of excited molecules, the luminescence light is emitted towards all directions with the same probability. Therefore, some portion of light would leave the gas bubble immediately after emission. This can explain the fact that the radiation peak of SL and the peak of reference radiation from the mercury–argon lamp are superimposed on each other [35].

A significant part of luminescent radiation of the gas is reflected from the walls of the expanding bubble and its frequency decreases proportionally to the number of reflections from the inner walls of the bubble. Some portion of the emitted light falls on the inner walls of the bubble at the angles greater than the critical angle of total reflection. The number of reflections of this light from the inner walls depends on the initial incidence angle. The larger the angle φ in Fig. 4, the more reflections occur inside the expanding bubble. Consequently, the later this light leaves the

expanding bubble, the more noticeable the 'red' shift of this spectrum is. This imposes the fact that the peaks in the SL spectrum become asymmetric and their low-frequency side becomes wider than the high-frequency one.

Large population of high-energy levels in the gas filling the bubble at the final stage of its collapse can be linked with the differences between the spectra of single- and multi-bubble SLs. As shown above, in addition to blackbody-like spectral continuum, there are the emission lines of hydroxyl OH* (at 310 nm) and Na⁺ ion in the spectrum of multi-bubble SL [11]. On the other hand, these lines are absent in the spectrum of single-bubble SL taking place in the same NaCl solution in water and under the same other conditions [11]. This peculiarity can be explained as follows. When the light emitted by a single gas bubble passes through another gas bubble with a large population of high-energy levels, induced emission of light and transitions of excited electrons to their ground states can happen. When the light passes through a sequence of neighbouring bubbles, it is amplified precisely at those frequencies which correspond to the excited states. This process gives rise to the peaks corresponding to the energies of excited states against the background of continuous spectrum typical for the blackbody.

6. Conclusions

We have offered a new theoretical model for the SL effect. According to this model, multiple reflections of infrared radiation occur inside a collapsing gas bubble and the wavelength of thermal radiation decreases slightly at each reflection from the inner walls of the bubble. As we have demonstrated, only a few nanoseconds are sufficient for essential total decrease in the wavelength of thermal radiation.

Our model of the SL emission provides non-contradictory explanations for the following features of the SL, which have been confirmed experimentally in the earlier studies:

- a short bright flash of light happens at the moment when the radius of the collapsing bubble reaches its minimum;
- a clear conformability of the SL spectrum with the spectra peculiar for the blackbody radiation;
- extremely high temperatures corresponding to the SL spectrum;
- an increase in the SL intensity detected under conditions when the water or the other liquids are saturated with noble gases;
- an influence of water temperature on the SL intensity;
- a presence of the emission bands in the SL spectrum, which correspond to abnormally high-energy levels and cannot be excited thermally;
- differences detected in the spectra of single- and multi-bubble SLs;
- a 'red' shift and asymmetry of the emission bands of gas molecules occurring during the SL.

Further experimental confirmations of our SL model are needed. Note also that, in case if our model will have become firmly substantiated, it can open up a number of novel possibilities for improving lasers and some other optical devices.

References

1. Marinenco M and Trillal Y Y, 1933. Acton des ultrasons sur les plaques photographiques. C. R. Acad. Sci. Paris. **196**: 858–860.
2. Frenzel H and Schultes I, 1934. Luminescenz im ultraschallbeschickten Wasser. Z. Phys. Chem. B. **27**: 21–424.

3. Paounoff P, 1939. La luminescence de l'eau sous l'action des ultrasons. CR Hebd Séance Acad Sci. **209**: 33.
4. Gaitan D F and Crum L A, Frontiers of nonlinear acoustics. 12th ISNA. London: Elsevier Appl. Sci., 1990.
5. Gaitan D F, Grum L A, Church C C and Roy R A, 1992. Sonoluminescence and bubble dynamic for a single, stable cavitation bubble. J. Acoust. Soc. Amer. **91**: 3166–3183.
6. Hiller R, Putterman S J and Barber B P, 1992. Spectrum of synchronous picosecond sonoluminescence. Phys. Rev. Lett. **69**: 1182–1184.
7. Putterman S J and Weninger K R, 2000. Sonoluminescence: how bubbles turn sound into light. Ann. Rev. Fluid Mech. **32**: 445–476.
8. Hiller R, Weninger K, Putterman S J and Barber B P, 1994. Effect of noble gas doping in single-bubble sonoluminescence. Science. **5183**: 248–250.
9. Barber B P, Hiller R A, Lofstedt R, Putterman S J and Weninger K R, 1997. Defining the unknowns of sonoluminescence. Phys. Rep. **281**: 65–143.
10. Flannigan D J and Suslick K S, 2005. Plasma formation and temperature measurement during single-bubble cavitation. Nature. **434**: 52–55.
11. Matula T J, Roy R A, Mourad P D, McNamara W B and Suslick K S, 1995. Comparison of multibubble and single-bubble sonoluminescence spectra. Phys. Rev. Lett. **75**: 2602–2605.
12. Didenko Y T and Gordeychuk T V, 2000. Multibubble sonoluminescence spectra in water which resemble single-bubble sonoluminescence. Phys. Rev. Lett. **84**: 5640.
13. Borisenok VA, 2015. Sonoluminescence: experiments and model (review). Acust. Zhurn. **61**: 333–360.
14. Margulis M A, 2000. Sonoluminescence. Soviet Phys.: Uspekhi. **43**: 259–282.
15. Young J B, Nelson J A and Kang W, 2001. Line emission in single-bubble sonoluminescence. Phys. Rev. Lett. **86**: 2673–2676.
16. Suslick K S and Flannigan D J, 2008. Inside a collapsing bubble: Sonoluminescence and the conditions during cavitation. Ann. Rev. Phys. Chem. **59**: 659–683.
17. McNamara W B, Didenko Y T and Suslick K S, 2003. Pressure during sonoluminescence. J. Phys. Chem. B. **107**: 7303–7306.
18. Kuhns D, Brodsky A and Burgess L, 1998. Hydrodynamical perturbation effects in multibubble sonoluminescence. Phys. Rev. E. **57**: 1702–1704.
19. Noltingk B E and Neppiras E A, 1950. Cavitation produced by ultrasonics. Proc. Phys. Soc. B. (London). **63B**: 674–685.
20. Neppiras E A and Noltingk B E, 1951. Cavitation produced by ultrasonics: theoretical conditions for the onset of cavitation. Proc. Phys. Soc. B. (London.) **64B**: 1032–1038.
21. Lykov A V. Theory of thermal conductivity. Moscow: Vysshaya Shkola, 1967.
22. Handbook of physical and technical fundamentals of cryogenics. Ed. by Malkov M P. Moscow: Energoatomizdat, 1985.
23. Moss W C, Clarke D B, White J W and Young D A, 1994. Hydrodynamic simulations of bubble collapse and picosecond sonoluminescence. Phys. Fluids. **6**: 2979–2985.
24. Weninger K, Putterman S J and Barber B P, 1996. Angular correlations in sonoluminescence: Diagnostic for the sphericity of a collapsing bubble. Phys. Rev. E. **54**: R2205–R2208.
25. Lepoint T, Pauw D D, Lepoint-Mullie F, Goldman M and Goldman A, 1997. Sonoluminescence: an alternative electrohydrodynamic hypothesis. J. Acoust. Soc. Amer. **101**: 2012–2030.

26. Prosperetti A J, 1997. New mechanism for sonoluminescence J. Acoust. Soc. Amer. **101**: 2003–2007.
27. Li J, Liu L, Tang J, Li G, Ma H, Gu Y, Liu S, Weng J and Chen Q F, 2018. Refractive index measurement of compressed nitrogen using an infrared frequency-domain interferometer. Optik. **164**: 1–4.
28. Thormählen I, Straub J and Grigull U, 1985. Refractive index of water and its dependence on wavelength, temperature, and density. J. Phys. Chem. Ref. Data. **14**: 933–945.
29. Wanstall C T, Agrawal A K and Bittle J A, 2019. Implications of real-gas behavior on refractive index calculations for optical diagnostics of fuel-air mixing at high pressures. Comb. Flame. **214**: 47–56.
30. Flannigan D J, Hopkins S D, Camara C G, Putterman S J and Suslick K S, 2006. Measurement of pressure and density inside a single sonoluminescing bubble. Phys. Rev. Lett. **96**: 204301.
31. Sonoluminescence. Movie from UCLA Putterman group. URL: <https://www.youtube.com/watch?v=rhiaFa9kaH4>
32. Feynman R P, Leighton R B and Sands M. The Feynman lectures on physics. Vol. 1. Massachusetts: Addison-Wesley, 1977.
33. Sivukhin D V. A course of general physics. Vol. 4. Optics. Moscow: Fizmatlit, 2002.
34. Young F R. Sonoluminescence. Boca Raton, Florida: CRC Press LLC, 2000.
35. Flannigan D J and Suslick K S, 2010. Inertially confined plasma in an imploding bubble. Nature Phys. **6**: 598–601.

Kravchenko M. B. 2022. A new possible model of sonoluminescence. Ukr.J.Phys.Opt. **23**: 37 – 55. doi: 10.3116/16091833/23/1/37/2022

***Анотація.** Запропоновано нову теоретичну модель для ефекту сонолюмінесценції (СЛ). Відповідно до цієї моделі, всередині газової бульбашки, яка колапсує, можуть сформуватися умови для повного внутрішнього відбивання світла. Завдяки цьому на внутрішній поверхні бульбашки мають місце багатократні відбивання видимого світла та інфрачервоного випромінювання. Після кожного відбивання від стінок бульбашки відбувається незначне зменшення довжини хвилі теплового випромінювання. На конкретному прикладі продемонстровано, що лише кількох наносекунд достатньо, аби довжина хвилі теплового випромінювання всередині бульбашки істотно зменшилася. Наша модель дає змогу пояснити основні особливості СЛ: спектр випромінювання, який відповідає спектрові абсолютно чорного тіла з надзвичайно високою температурою, роль благородних газів у зростанні яскравості СЛ, а також вплив температури води на яскравість СЛ.*